SIAM REVIEW
Vol. 43, No. 2, pp. 315–344

© 2001 Society for Industrial and Applied Mathematics

Synchronization of Elliptic Bursters*

Eugene M. Izhikevich†

Abstract. Periodic bursting behavior in neurons is a recurrent transition between a quiescent state and repetitive spiking. When the transition to repetitive spiking occurs via a subcritical Andronov–Hopf bifurcation and the transition to the quiescent state occurs via fold limit cycle bifurcation, the burster is said to be of *elliptic* type (also known as a "subHopf/fold cycle" burster). Here we study the synchronization dynamics of weakly connected networks of such bursters. We find that the behavior of such networks is quite different from the behavior of weakly connected phase oscillators and resembles that of strongly connected relaxation oscillators. As a result, such weakly connected bursters need few (usually one) bursts to synchronize, and synchronization is possible for bursters having quite different quantitative features. We also find that interactions between bursters depend crucially on the spiking frequencies. Namely, the interactions are most effective when the presynaptic interspike frequency matches the frequency of postsynaptic oscillations. Finally, we use the FitzHugh–Rinzel, Morris–Lecar, and Hodgkin–Huxley models to illustrate our major results.

Key words. subcritical elliptic burster, normal form, slow passage effect, fast threshold modulation, FM interactions

AMS subject classifications. 92B20, 92C20, 82C32, 58Fxx, 34Cxx, 34Dxx

PII. S0036144500382064

1. Introduction.

This article is a revised and condensed reprint of the paper "Subcritical Elliptic Bursting of Bautin Type" (Izhikevich (2000b)). The following important modifications have been made to make the subject more accessible to readers:

- The introduction section is significantly extended.
- Technical theorems and proofs are omitted.
- Simulations of Hodgkin–Huxley-type models are included to illustrate major theoretical results.

Coupled elliptic bursters provide a unique example of a bursting network whose synchronization dynamics can be analyzed and understood in a quite general setting without resort to computer simulations. An interested reader could learn more about nonlinear dynamics and bursting in neurons in the review/tutorial paper "Neural Excitability, Spiking, and Bursting" (Izhikevich (2000a)), which contains 126 color illustrations.

1.1. Bursters.

Periodic bursting behavior in neurons is a recurrent transition between a quiescent state and a state of repetitive firing, as we illustrate in Figure 1.1.

*Published electronically May 2, 2001. This paper originally appeared in *SIAM Journal on Applied Mathematics*, Volume 60, Number 2, 2000, pages 503–535.
http://www.siam.org/journals/sirev/43-2/38206.html

†The Neurosciences Institute, 10640 John Jay Hopkins Drive, San Diego, CA 92121 (Eugene. Izhikevich@nsi.edu, http://www.nsi.edu/users/izhikevich).

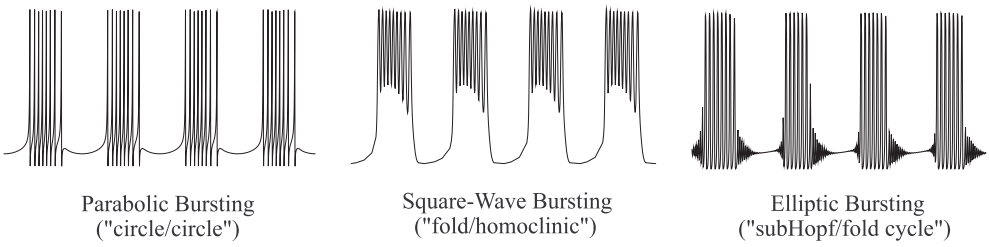

Fig. 1.1 *Major types of bursters (modified from Hoppensteadt and Izhikevich* (1997)*).*

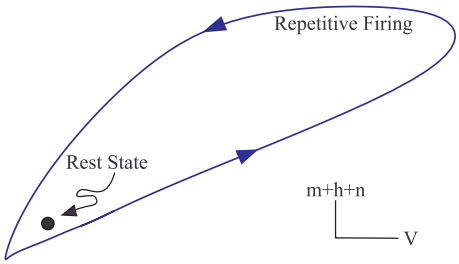

Fig. 1.2 *Projection of a periodic solution* $(I = 7)$ *and a quiescent solution* $(I = 0)$ *of the Hodgkin–Huxley model on the plane* $(V, m + h + n)$*.*

Many mathematical models of bursters can be written in the singularly perturbed form

$$\begin{aligned} \dot{x} &= f(x, y), \\ \dot{y} &= \mu g(x, y), \end{aligned} \tag{1.1}$$

where $x \in \mathbb{R}^m$ is a vector of fast variables responsible for repetitive firing. It accounts, e.g., for the membrane voltage and fast currents. The vector $y \in \mathbb{R}^k$ is a vector of slow variables that modulates the firing. It accounts, e.g., for slow (in)activation dynamics and changes in intracellular Ca^{2+} concentration. We provide some typical examples below. The small parameter $\mu \ll 1$ is a ratio of fast/slow time scales.

1.2. Classification. First, let us consider the fast subsystem $\dot{x} = f(x, y)$ alone and treat y as a bifurcation parameter. This is a standard approach known as dissection of bursting (Rinzel and Lee (1987)). The silent phase of the burster corresponds to x being at an equilibrium. The repetitive spiking corresponds to x being on a limit cycle; see Figure 1.2. As y changes slowly, the attractors of the fast subsystem bifurcate. Among many possible bifurcations there are two, depicted in Figure 1.3, that define the type of burster:

- The bifurcation of the rest state that corresponds to the transition from quiescence to repetitive firing. This bifurcation determines how the firing appears.
- The bifurcation of the limit cycle that corresponds to the transition from repetitive firing to rest. This bifurcation determines how the firing disappears.

A partial classification of bursters based on these bifurcations was provided by Rinzel (1987), Wang and Rinzel (1995), Bertram et al. (1995), and Hoppensteadt and Izhikevich (1997, section 2.9.5). It is summarized in Figure 1.4.

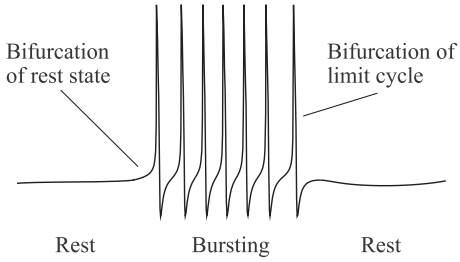

Fig. 1.3 *Two important bifurcations associated with bursting (modified from Izhikevich* (2000a)).

Bifurcations	*Saddle-Node on Invariant* **Circle**	*Saddle* **Homoclinic** *Orbit*	*Supercritical Andronov–* **Hopf**	**Fold** *Limit* **Cycle**
Fold	triangular	square-wave Type I	tapered Type V	Type IV
Saddle-Node on Invariant **Circle**	parabolic Type II			
Supercritical Andronov– **Hopf**				
Sub*critical Andronov–* **Hopf**				elliptic Type III

Fig. 1.4 *Bifurcation mechanisms of classical bursters. Left column: List of bifurcations from rest to repetitive spiking. Top row: List of bifurcations from repetitive spiking to rest; see Figure* 1.3 *(modified from Izhikevich* (2000a)).

A complete classification of bursters of the form (1.1) was provided by Izhikevich (2000a). For example, when the fast subsystem in (1.1) is planar (i.e., $m = 2$), there could be four codimension-1 bifurcations of an equilibrium and four codimension-1 bifurcations of a limit cycle attractor. Any combination of them would result in a different type of bursting. Hence there are sixteen types of such planar bursters, which are summarized in Figures 1.5 and 1.6.

It is convenient to name the bursters after the two bifurcations involved. For example, the parabolic burster has an alternative name, "circle/circle," because both bifurcations are of saddle-node on invariant *circle* type. The square-wave burster has an alternative name, "fold/homoclinic," because the rest activity disappears via *fold* bifurcation and the repetitive firing disappears via saddle *homoclinic* orbit bifurcation.

In this paper we study elliptic bursting, which has an alternative name, "sub-Hopf/fold cycle," because the rest state loses stability via *sub*critical Andronov–*Hopf*

Bifurcations	*Saddle-Node on Invariant* **Circle**	*Saddle* **Homoclinic** *Orbit*	*Supercritical Andronov–* **Hopf**	**Fold** *Limit* **Cycle**
Fold	fold/ circle	fold/ homoclinic	fold/ Hopf	fold/ fold cycle
Saddle-Node on Invariant **Circle**	circle/ circle	circle/ homoclinic	circle/ Hopf	circle/ fold cycle
Supercritical Andronov– **Hopf**	Hopf/ circle	Hopf/ homoclinic	Hopf/ Hopf	Hopf/ fold cycle
Sub*critical Andronov–* **Hopf**	subHopf/ circle	subHopf/ homoclinic	subHopf/ Hopf	subHopf/ fold cycle

Fig. 1.5 *A classification of codimension-*1 *planar fast/slow point-cycle bursters (modified from Izhikevich* (2000a)*). Each burster is named after the two bifurcations. See also Figure* 1.6.

bifurcation and the limit cycle attractor disappears via *fold* limit *cycle* bifurcation (also known as double limit cycle, saddle-node or fold of limit cycles). Both bifurcations, illustrated in Figure 1.7, are ubiquitous in neural systems. The burster's phase portrait is depicted in Figure 1.8. Since there is a coexistence of rest and limit cycle attractors, the periodic transition between them often occurs via a hysteresis loop, as we illustrate in Figure 1.9.

A distinctive feature of elliptic bursting is that the frequency of spiking, which we denote by Ω in this paper, is relatively constant, while the amplitude may change significantly.

1.3. Examples. Elliptic bursting is ubiquitous in Hodgkin–Huxley-type electrophysiological models. It can even be generated by the classical Hodgkin–Huxley (1954) model, as we illustrate in Figure 1.10. Moreover, there are two ways to make the Hodgkin–Huxley model burst.

In Figure 1.10a we change the time scale of inactivation of the Na^+ current, so that the Hodgkin–Huxley model can be written in the form (1.1) with $x = (V, m, n)$ and $y = h$ (here V is the membrane potential and m, n, and h are gating variables in the Hodgkin–Huxley model). Action potentials are generated via the interplay between fast activation of Na^+ and K^+ currents. (In this case the fast subsystem is equivalent to the Morris–Lecar (1981) model.) The active phase of bursting terminates because of the slow inactivation of the Na^+ current.

In Figure 1.10b we change the time scale of activation of the K^+ current, so that $x = (V, m, h)$ and $y = n$ in (1.1). Action potentials are generated via the interplay between activation and inactivation of the Na^+ current. The active phase of bursting terminates because of the slow activation of the outward K^+ current.

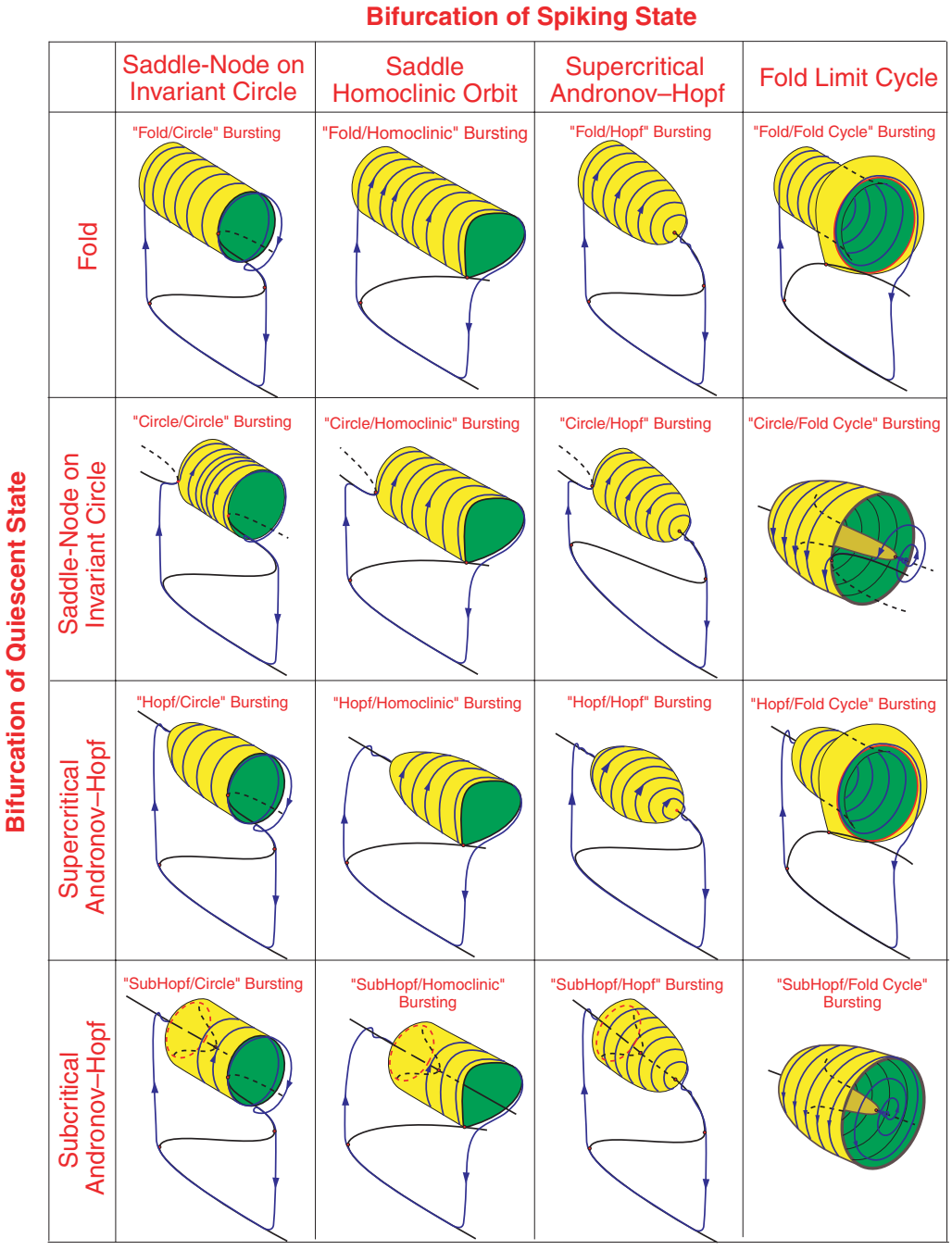

Fig. 1.6 *Possible phase portraits of planar bursters from Figure* 1.5 *(from Izhikevich* (2000a)*). Reprinted with permission from World Scientific Publishing.*

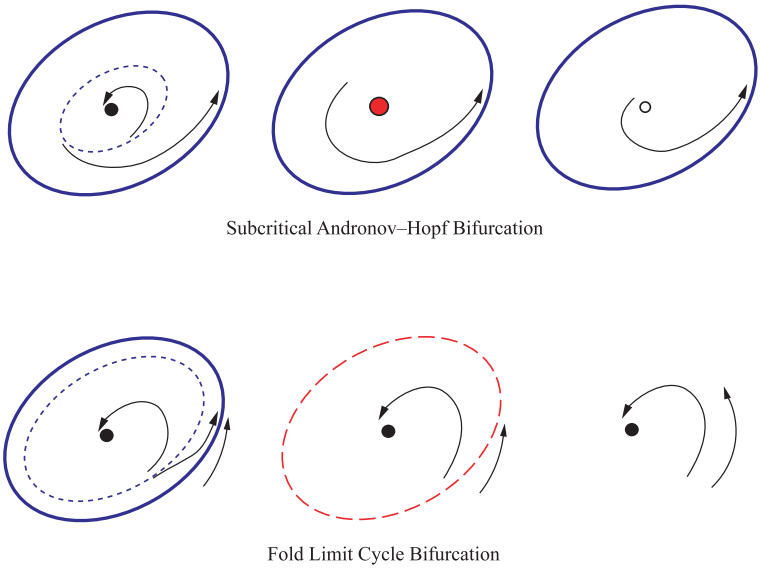

Fig. 1.7 *Major bifurcations in the elliptic ("subHopf/fold cycle") bursting.*

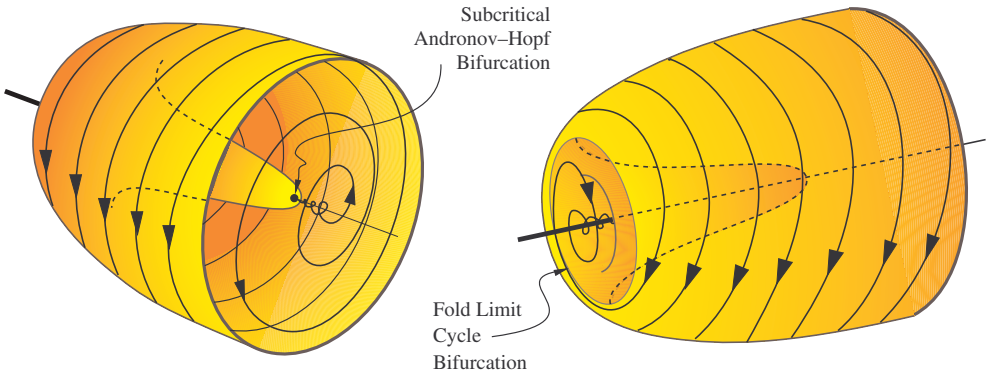

Fig. 1.8 *Elliptic ("subHopf/fold cycle") burster. The rest state loses stability via subcritical Andronov–Hopf bifurcation and the limit cycle disappears via fold limit cycle bifurcation (from Hoppensteadt and Izhikevich* (1997)*).*

In both cases the repetitive firing starts via subcritical Andronov–Hopf bifurcation and terminates via fold limit cycle bifurcation. Hence, the bursting is elliptic ("subHopf/fold cycle").

Many examples of bursting systems can be constructed as follows: Take a neural model whose bifurcation structure is understood and use it as the fast subsystem in (1.1). Then, add a slow subsystem that drives the model through the desired bifurcations. For example, in Figure 1.11 we take the Morris–Lecar (1981) model which has nullclines (green curves) intersected in one point as shown in the insets. The model exhibits bistability of equilibrium (black dot) and limit cycle (blue loop) attractors separated by an unstable limit cycle (blue dashed loop). Changing param-

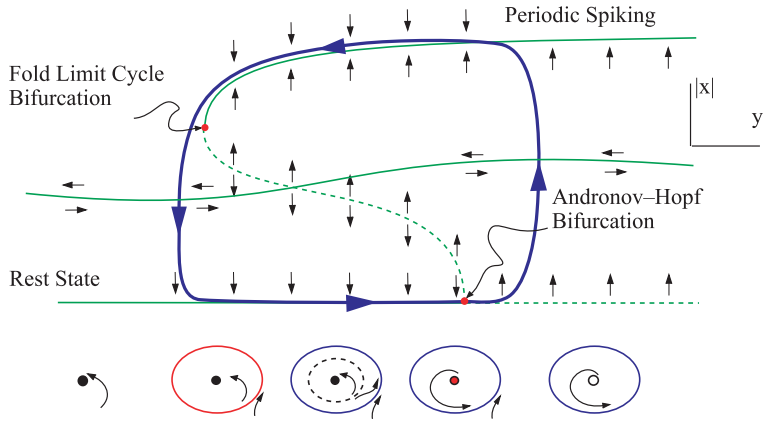

Fig. 1.9 *Elliptic bursting may occur via a hysteresis loop.*

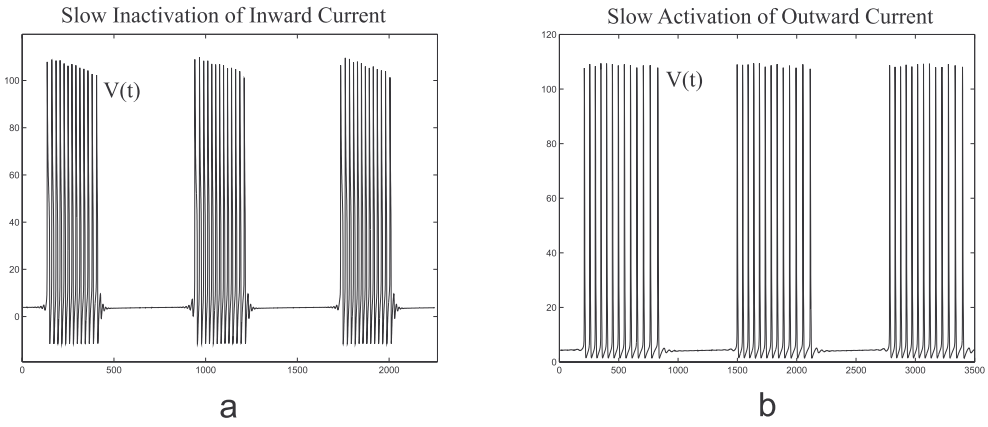

Fig. 1.10 *Elliptic ("subHopf/fold cycle") bursting in the classical Hodgkin–Huxley* (1954) *model (variables V, m, h, n) having original values of parameters with the following exceptions:* (a) $\alpha_n(V)$ *and* $\bar{g}_{\mathrm{Na}}$ *are half the original values,* $\alpha_h(V)$ *is four times the original value,* $\beta_n(V) = 0.125e^{-V/10}$, *and the equation for* h' *is multiplied by* 0.01 *(inactivation of* I_{Na} *is slow).* (b) $I = 5.46$, $\alpha_n(V)$ *is* 0.6 *of the original value,* $\alpha_h(V) = 0.07e^{-V/12}$, *and the equation for* n' *is multiplied by* 0.0001 *(activation of* I_{K} *is slow). Notice that no additional ions or currents were used.*

eters, e.g., the value of the injected current, drives the system through subcritical Andronov–Hopf bifurcation or fold limit cycle bifurcation. Now we assume that the injected current is a slow variable that depends on membrane voltage. For example, it could be a slow voltage-gated K^+ outward current (there are many other choices). Quiescent dynamics result in decrease of the outward current, and the Morris–Lecar model starts to fire spikes. Spiking dynamics slowly increase the outward current, and the model becomes quiescent. Recurrent transition between quiescence and repetitive spiking results in the bursting dynamics depicted in Figure 1.11. Incidentally, this mechanism is believed to be responsible for the elliptic bursting in the primary afferent neurons in the brain stem circuits (Pedroarena et al. (1999)).

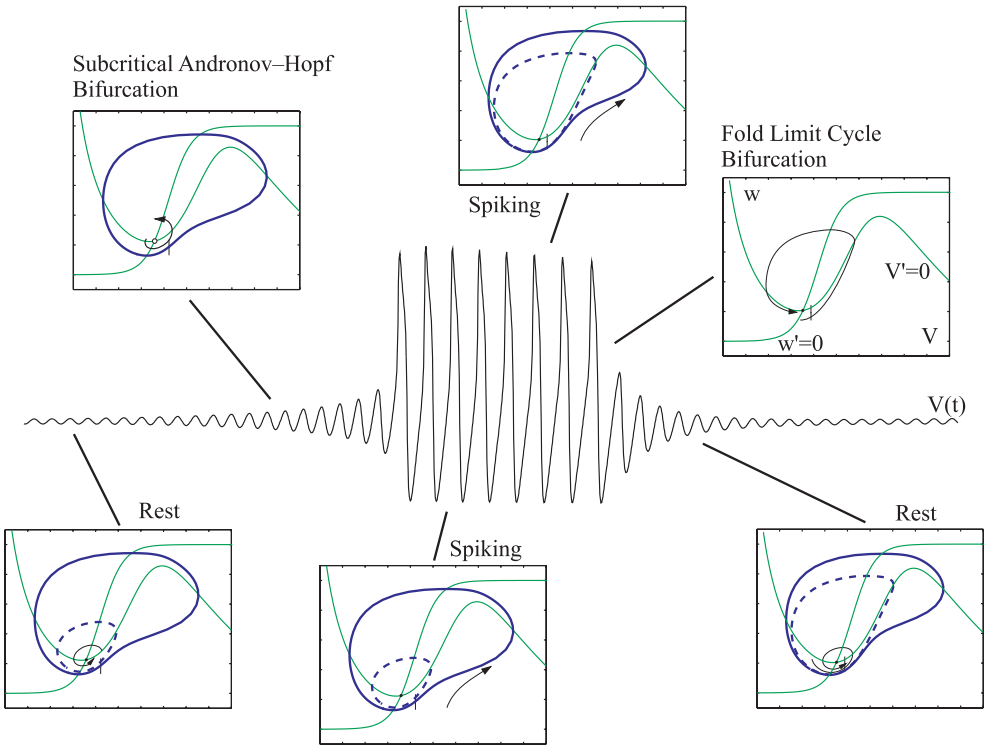

Fig. 1.11 *Elliptic bursting in the Morris–Lecar* (1981) *system (variables V and w) with an additional slowly activated outward current. Green curves are nullclines $V' = 0$ and $w' = 0$ of the fast subsystem.*

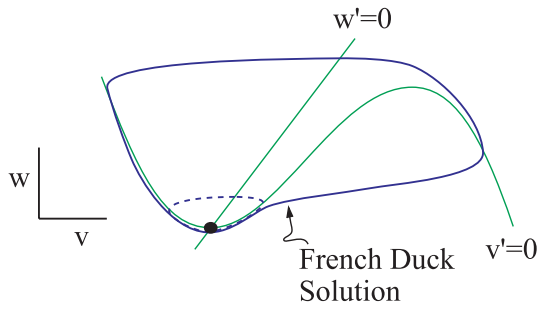

Fig. 1.12 *Nullclines, stable, and unstable limit cycles of the FitzHugh–Nagumo model.*

1.4. Singular Hopf Bifurcations and Duck Solutions. When the fast subsystem $\dot{x} = f(x, y)$ has many time scales, it can generate action potentials via relaxation oscillations. A typical example is the FitzHugh–Nagumo model (FitzHugh (1961))

$$\begin{aligned} \dot{v} &= v - v^3/3 - w + y, \\ \dot{w} &= \delta(a + v - bw) \end{aligned}$$

for $a = 0.7,\ b = 0.8$, and $\delta \ll 1$, whose nullclines are depicted in Figure 1.12.

If we vary the bifurcation parameter y, the FitzHugh–Nagumo model may undergo subcritical Andronov–Hopf or fold limit cycle bifurcation. A nasty problem associated with the Andronov–Hopf bifurcation in the system above is that the bifurcation is *singular* (Baer and Erneux (1986), (1992); Arnold et al. (1994)); that is, the pure imaginary eigenvalues of the Jacobian matrix at the bifurcation point have infinitesimal imaginary parts (of order $\sqrt{\delta}$). This complicates the analysis substantially, since many singular phenomena may appear, such as nonsmooth (triangular) limit cycles, French duck solutions (Eckhaus (1983)), steep growth of amplitude of oscillation, enormous disparity of interspike frequency and the frequency of small amplitude oscillations, etc.

An elliptic burster is referred to as being *singular* if the fast subsystem is of relaxation type having singular Andronov–Hopf bifurcation, and the fold limit cycle bifurcation occurs in the French duck territory. A typical example of a singular elliptic burster is the FitzHugh–Rinzel model, which we consider in section 5.

1.5. Bautin Bifurcation. In what follows we assume that even when the fast subsystem has many time scales, the Andronov–Hopf bifurcation is *regular* (i.e., the pure imaginary eigenvalues of the Jacobian matrix at the bifurcation point have nonvanishing imaginary parts) and the limit cycles are smooth. We refer to such elliptic bursters as *Bautin bursters* due to the reason explained below.

Since the Andronov–Hopf and fold limit cycle bifurcations have codimension 1 (Kuznetsov (1995)), the corresponding bifurcation sets of the dynamical system $\dot{x} = f(x, y)$ in the parameter space $\mathbb{R}^k \ni y$ are $(k-1)$-dimensional hypersurfaces. In particular, they are curves when $y \in \mathbb{R}^2$; see the lower part of Figure 1.13.

Repetitive bursting occurs when the slow variable y crosses the curves periodically. When the curves are far away from each other, variable y oscillates with large amplitude, and we call such a Bautin burster *global*; see Figure 1.13. Quite often, however, the curves meet tangentially at a point at which a Bautin bifurcation occurs (Kuznetsov (1995)). This bifurcation, also known as a degenerate or generalized Hopf bifurcation, has codimension 2, and it can be observed in many neural models, for example, in the Wilson–Cowan oscillator (Borisyuk and Kirillov (1992), Hoppensteadt and Izhikevich (1997)). When the fast subsystem is near the Bautin bifurcation point so that the slow variable y has small amplitude oscillations, the burster is said to be *local*; see Figure 1.13. This is the type of elliptic bursting we study in this paper; see the summary in Figure 1.14.

Any dynamical system at the Bautin bifurcation can be transformed by a suitable continuous change of variables into its topological normal form (see Kuznetsov (1995))

$$\dot{z} = (l_0 + \mathrm{i}\Omega)z + l_1 z|z|^2 + l_2 z|z|^4 \,, \tag{1.2}$$

where $z \in \mathbb{C}$ is a complex variable, $\Omega > 0$ is the imaginary part of the complex-conjugate eigenvalue at the Bautin point, and l_0, l_1, and l_2 are real parameters. The last two are called first and second *Liapunov coefficients*, respectively. The Bautin bifurcation occurs when

$$l_0 = l_1 = 0 \qquad \text{but} \qquad l_2 \neq 0 \,.$$

When $l_2 < 0$ ($l_2 > 0$), the Bautin bifurcation is said to be supercritical (subcritical), and the large-amplitude limit cycle corresponding to the spiking state (blue circle in Figure 1.13) is stable (unstable). From now on we consider only supercritical Bautin bifurcations.

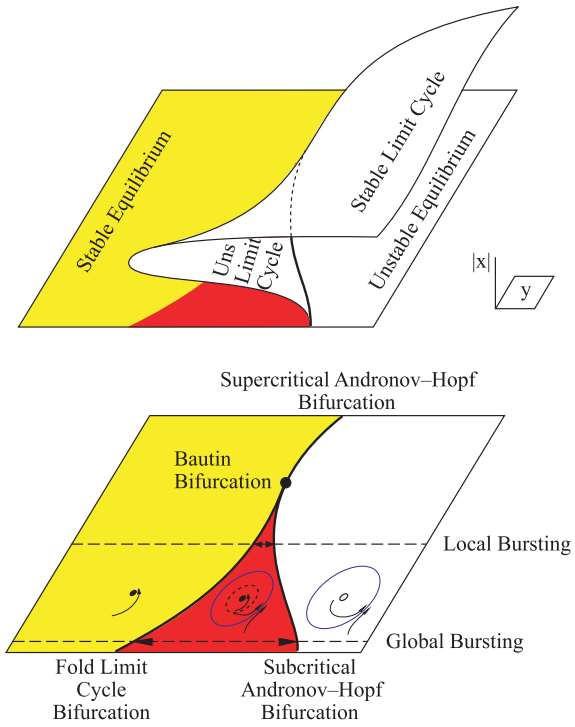

Fig. 1.13 *A neighborhood of a supercritical Bautin bifurcation. The yellow area denotes the region of stability of the equilibrium corresponding to the rest state. The red area denotes the region of bistability of the equilibrium and a limit cycle attractor corresponding to the periodic firing.*

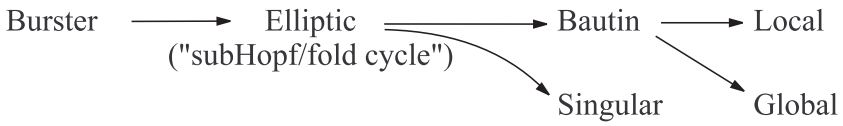

Fig. 1.14 *A partial classification of elliptic ("subHopf/fold cycle") bursters.*

It is easy to see that (1.2) undergoes Andronov–Hopf bifurcation for $l_0 = 0$, which is supercritical for $l_1 < 0$ and subcritical otherwise. Moreover, if $l_1 > 0$, then (1.2) undergoes fold limit cycle bifurcation when

$$l_1^2 - 4l_0l_2 = 0; \tag{1.3}$$

see Figure 1.15. We see that both Andronov–Hopf and fold limit cycle bifurcations occur simultaneously at the Bautin point $l_0 = l_1 = 0$. In any case variable z exhibits damped or sustained oscillations with frequency $\Omega > 0$.

The assumption that bifurcations leading to the appearance and disappearance of periodic spiking in the fast system occur for nearby values of the slow variable y is not new in mathematical neuroscience. It has been used successfully by Ermentrout and Kopell (1986a), (1986b) in their study of parabolic bursters. Their major achievement

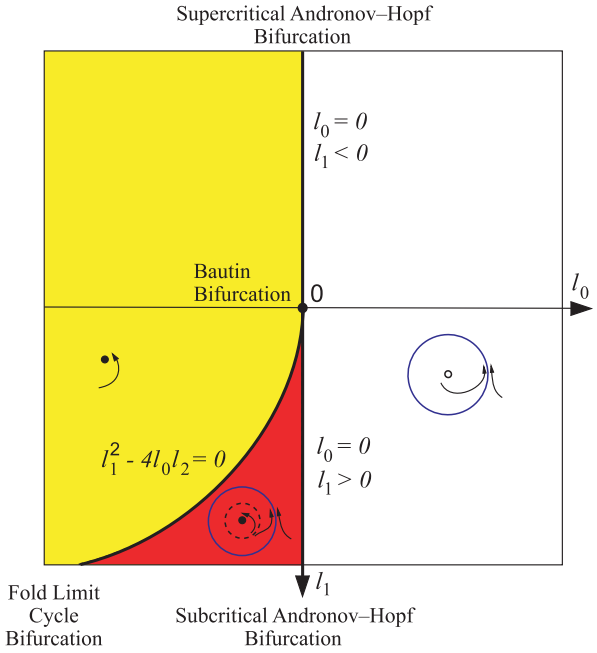

Fig. 1.15 *Supercritical Bautin bifurcation in* (1.2). *Note that the positive* l_1 *axis points downward so that relevant regions are oriented the same way as in Figure* 1.13.

was derivation of the canonical model for local parabolic bursters. In this paper we derive a canonical model for local Bautin bursters.

2. Canonical Model. One can easily study a model of an elliptic burster by assuming that the functions f and g in (1.1) have a certain "biologically plausible" form. A potential problem is that the biological plausibility of f and g might be only an illusion. Moreover, the results predicted by the model might disappear when f and g are adjusted to take into account more biological data. To avoid this kind of problem Hoppensteadt and Izhikevich (1997) developed a canonical model approach, which can be summarized as follows: Instead of studying (1.1) for some f and g, let us consider all possible f and g satisfying only a few general assumptions, e.g., that the burster is local. Then we seek a continuous (possibly noninvertible) change of variables that puts (1.1) for all such f and g into a simpler model, which is called *canonical*.

THEOREM 2.1 (canonical model for Bautin bursters). *Consider* (1.1) *having a fast subsystem in an* ε*-neighborhood of the Bautin bifurcation point. There is a continuous change of variables that transforms all such* (1.1) *into the canonical model*

$$\begin{aligned} z' &= (u + i\omega)z + 2z|z|^2 - z|z|^4 \\ u' &= \eta(a - |z|^2) \end{aligned} \quad + \ \mathcal{O}(\sqrt[4]{\varepsilon}) \,, \tag{2.1}$$

where $' = d/d\tau$, $\tau = \mathcal{O}(\varepsilon)t$ *is slow time,* $z \in \mathbb{C}$ *and* $u \in \mathbb{R}$ *are new fast and slow variables, respectively, and* $a, \omega \in \mathbb{R}$ *and* $\eta = \mathcal{O}(\mu/\varepsilon^{3/2})$ *are parameters.*

Nonzero values of $z(\tau)$ correspond to periodic spiking of the fast variable $x(t)$ with amplitude of order $\sqrt[4]{\varepsilon}|z|$ and interspike frequency of order Ω (see Figure 2.1), where $\pm i\Omega$ are the pure imaginary eigenvalues of the fast subsystem $\dot{x} = f(x, y)$ at the

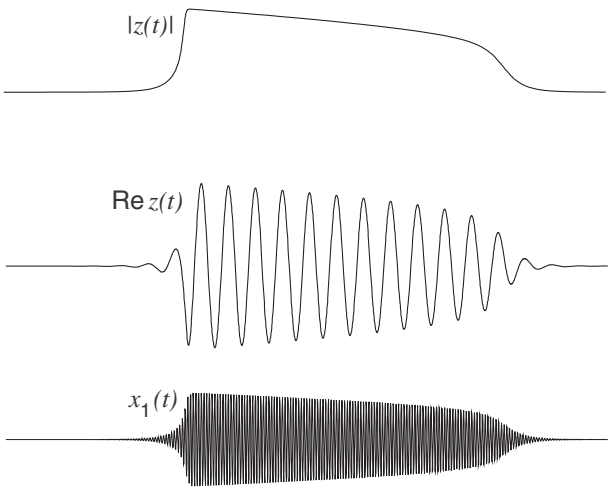

Fig. 2.1 *The relationship between* $z \in \mathbb{C}$ *and* $x \in \mathbb{R}^m$ (*simulation parameters:* $a = 0.8,\ \eta = \varepsilon = 0.1,\ \Omega = \omega = 3,\ t \in [0, 500]$).

Bautin point. The canonical model (2.1) exhibits bursting when $\eta \ll 1$ and $0 < a < 1$. It exhibits tonic spiking when $a > 1$.

As expected, the fast subsystem in the canonical model (2.1) is similar to the topological normal form for Bautin bifurcation (1.2). The coefficient 2 in the term $2z|z|^2$ is chosen for the sake of convenience so that the fast subsystem undergoes Andronov–Hopf and fold limit cycle bifurcations for $u = 0$ and $u = -1$, respectively. The form of the slow subsystem might seem unexpected, since it depends neither on u nor on z or $\bar{z}$ in the first order. Detailed derivation of this equation can be found in Izhikevich (2000b). We just mention here that u disappears because the slow variable y oscillates with much smaller amplitude than that of x. Moreover, the frequency of x is much higher than that of y; therefore, any term that depends on the phase of x averages out, which leaves only $|z|^2$.

Finally, we notice that particulars of f and g do not affect the form of the canonical model but affect only the values of parameters η and a. Thus, studying (2.1) for all a and η, which we do below, sheds some light on dynamic behavior of all local Bautin bursters of the form (1.1) including those that have not been invented yet.

2.1. Analysis of the Canonical Model. Let $r = |z|$ denote the amplitude of oscillation of the fast variable $z \in \mathbb{C}$. We neglect the term $\mathcal{O}(\sqrt[4]{\varepsilon})$ and rewrite the canonical model (2.1) in the form

$$\begin{aligned} r' &= ur + 2r^3 - r^5, \\ u' &= \eta(a - r^2). \end{aligned} \tag{2.2}$$

Nontrivial ($r \neq 0$) equilibria of this system correspond to limit cycles of the canonical model (2.1), which may look like periodic (tonic) spiking with frequency ω. Limit cycles of this system correspond to periodic or quasi-periodic solutions of (2.1), which look like bursting; see Figure 2.2.

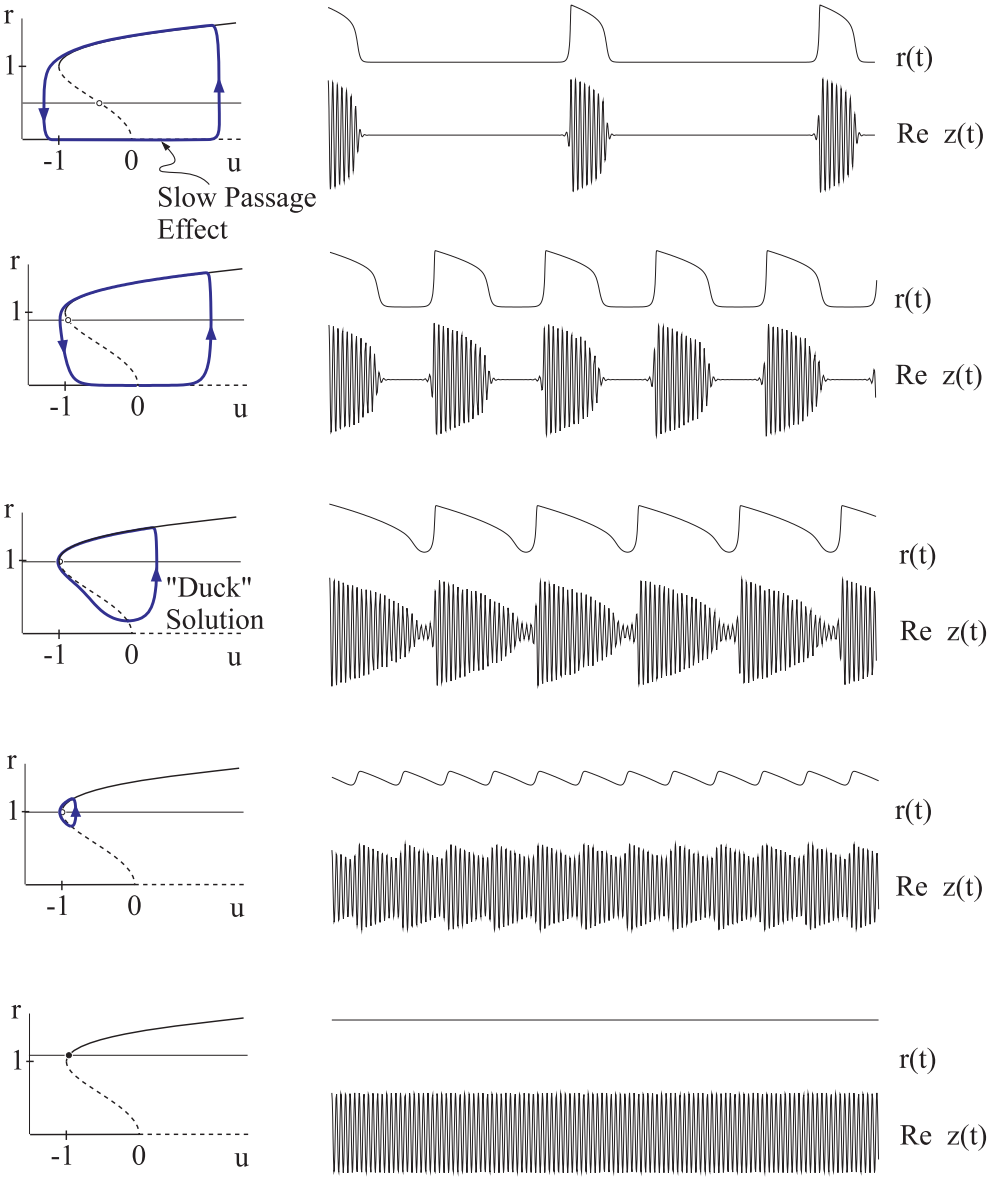

Fig. 2.2 *Phase portrait and solution of the canonical model* (2.2) *for* $\eta = 0.1$, $\omega = 3$, *and various* a. *From top to bottom:* $a = 0.25$, $a = 0.8$, $a = 0.986$, $a = 0.987$, *and* $a = 1.2$.

System (2.2) has a unique equilibrium,

$$\begin{pmatrix} r \\ u \end{pmatrix} = \begin{pmatrix} \sqrt{a} \\ a^2 - 2a \end{pmatrix}$$

for all η and $a > 0$, which is stable when $a > 1$. When a decreases and passes an η-neighborhood of $a = 1$, the equilibrium loses stability via a singular Hopf bifurcation (Baer and Erneux (1986), (1992); Arnold et al. (1994)). Among many interesting features of this bifurcation is the existence of French ducks (canards); see Eckhaus

(1983) and the middle part of Figure 2.2. When $0 < a < 1$, the system (2.2) has a limit cycle attractor. Therefore, the canonical model (2.1) and the original system (1.1) exhibit bursting behavior; see the upper part of Figure 2.2. The smaller a is, the longer is the interburst period. When $a \to 0$, the interburst period becomes infinite.

Notice that the system (2.2) cannot be used to completely analyze the behavior of the canonical model (2.1) for $a \approx 1$ or $a \approx 0$ since small terms hidden in $\mathcal{O}(\sqrt[4]{\varepsilon})$ might not be negligible in this case.

3. Weakly Connected Networks. Weakly connected networks of bursters can be written in the "weakly connected" form

$$\begin{aligned} \dot{x}_i &= f_i(x_i, y_i) + \varepsilon p_i(x, y, \varepsilon), \\ \dot{y}_i &= \mu\{g_i(x_i, y_i) + \varepsilon q_i(x, y, \varepsilon)\}, \end{aligned} \tag{3.1}$$

where each pair $(x_i, y_i) \in \mathbb{R}^m \times \mathbb{R}^k$ describes the activity of the ith burster, the functions p_i and q_i define how the bursters interact, and the parameter $\varepsilon \in \mathbb{R}$ is small, reflecting the strength of connections in the network. Hoppensteadt and Izhikevich (1997) obtained the estimate

$$0.004 < \varepsilon < 0.008$$

using experimental data from the hippocampus (McNaughton, Barnes, and Andersen (1981)).

It is a daunting task to study (3.1) without even knowing how p_i and q_i look. We use the assumption $\varepsilon \ll 1$ to achieve this goal. In Izhikevich (2000b) we showed that (3.1), satisfying a few additional assumptions, can be transformed into the canonical model (3.2).

THEOREM 3.1 (canonical model for weakly connected local Bautin bursters). *Consider a network of weakly connected local Bautin bursters* (3.1) *having interspike frequencies* $\Omega_i + \varepsilon\omega_i$. *There is an* $\varepsilon_0 > 0$ *such that for all* $\varepsilon \le \varepsilon_0$ *there is a continuous change of variables that transforms the network into the canonical model*

$$\begin{aligned} z_i' &= (b_i u_i + \mathrm{i}\omega_i) z_i + c_i z_i |z_i|^2 - d_i z_i |z_i|^4 + \textstyle\sum_{j=1}^{n} c_{ij} z_j \\ u_i' &= \eta_i (a_i - |z_i|^2) \end{aligned} \quad + \mathcal{O}(\sqrt[4]{\varepsilon}), \tag{3.2}$$

where $' = d/d\tau$, $\tau = \varepsilon t$ *is slow time,* $z_i \in \mathbb{C}$ *and* $u_i \in \mathbb{R}$ *are new fast and slow variables describing the* i*th burster, respectively,* $\eta_i = \mathcal{O}(\mu_i/\varepsilon^{3/2})$, $a_i \in \mathbb{R}$, *and* $b_i, c_i, d_i \in \mathbb{C}$ *are parameters,* $i = 1, \dots, n$. *The synaptic coefficient* $c_{ij} \in \mathbb{C}$ *vanishes when the* i*th and the* j*th bursters have different natural interspike frequencies* Ω_i.

COROLLARY 3.2. *Since* $c_{ij} = 0$ *when* $\Omega_i \neq \Omega_j$, *local Bautin bursters do not interact unless they have matching interspike frequencies* Ω_i.

Thus, in order to establish communication, it is not enough to grow synaptic connections between such bursters; they must also establish a common interspike frequency. This mechanism resembles selective tuning in radio, and it seems to be a general principle of communication between weakly connected periodically spiking neurons (Hoppensteadt and Izhikevich (1996a), (1997), (1998); Izhikevich (1999)) or neurons having damped oscillations (Izhikevich (2000a)). Notice, though, that distinct *interburst* frequencies do not prevent the communication.

The corollary needs some adjustment when the interspike frequency depends essentially on the amplitude of spiking. We discuss this issue in section 5.3.

Remark 3.3. Even though we do not make any assumptions about the connection functions p_i and q_i in the weakly connected system (3.1), the connections between

bursters in the canonical model (3.2) become linear, where c_{ij} depend on the partial derivatives $D_{x_j} p_i$ at the Bautin bifurcation point. This is the consequence of the fact that each x_j oscillates with a small amplitude, therefore only linear terms are relevant up to the leading order.

Remark 3.4. It is not correct to assume that positive (negative) c_{ij} implies immediately that the synaptic connection between the corresponding bursters is excitatory (inhibitory). Each complex coefficient $c_{ij} = s_{ij} e^{\mathrm{i}\psi_{ij}}$ describes the amplitude and polarity of the connection, where $s_{ij} = |c_{ij}|$ gives the rescaled synaptic strength and $\psi_{ij} = \operatorname{Arg} c_{ij}$ encodes phase information about the synaptic connection, which we call the *natural phase difference* (Hoppensteadt and Izhikevich (1996a), (1997)). There we show that the relationship between c_{ij} and the sign of the synaptic connection is subtler than one might think.

We analyze the canonical model (3.2) below. We then compare its behavior with that of a network of FitzHugh–Rinzel, Morris–Lecar, and Hodgkin–Huxley bursters in section 5, and we discuss our findings in section 6.

4. Synchronization of Elliptic Bursters. There are two rhythmic processes associated with each burster: repetitive spiking and repetitive bursting. Therefore, there could be at least two different regimes of synchronization (see Figure 4.1):

- synchronization of individual spikes,
- synchronization of bursts.

As we will see below, one of them does not imply the other. Therefore, there is an additional regime in which both types of synchronization occur simultaneously (see, e.g., Figure 4.2). Whether or not a pair of bursters could synchronize depends on the burster types (Izhikevich (2000a)). For example, some bursters, such as parabolic ("circle/circle") bursters, are notorious for their resistance to any type of synchronization. Others, such as the elliptic burster studied in this paper, can easily exhibit spike and burst synchronization, as we show below.

4.1. Spike Synchronization. Synchronization of individual spikes within a single burst depends crucially on the interspike frequencies, and in general is difficult to achieve, since the interspike frequencies depend on the amplitudes of spikes $|z_i|$ (via $\operatorname{Im} c_i$ and $\operatorname{Im} d_i$) and the values of the slow variables u_i (via $\operatorname{Im} b_i$).

THEOREM 4.1 (spike synchronization of Bautin bursters). *If in the canonical model* (3.2) *all bursters have equal center frequencies* $\omega_1 = \cdots = \omega_n = \omega$, *the coefficients* b_i, c_i, *and* d_i *are real, and the matrix of synaptic connections* $C = (c_{ij})$ *is self-adjoint, i.e.,* $c_{ij} = \bar{c}_{ji}$, *then the firings of the fast variables* z_i *synchronize on a short time scale of order* 1. *More precisely, activity of the fast subsystem*

$$z_i' = (b_i u_i + \mathrm{i}\omega) z_i + c_i z_i |z_i|^2 - d_i z_i |z_i|^4 + \sum_{j=1}^{n} c_{ij} z_j$$

for $u_i = \text{const}$, $i = 1, \ldots, n$, *converges to a limit cycle.*

The proof follows from the existence of the energy function (Izhikevich (2000b))

$$E(z, \bar{z}) = -\sum_{i=1}^{n} \left(b_i u_i |z_i|^2 + \frac{c_i}{2} |z_i|^4 - \frac{d_i}{6} |z_i|^6 + \sum_{j=1}^{n} c_{ij} \bar{z}_i z_j \right).$$

Remark 4.2. Spike synchronization does not imply burst synchronization. Indeed, the result of the theorem above does not depend on the values of the real

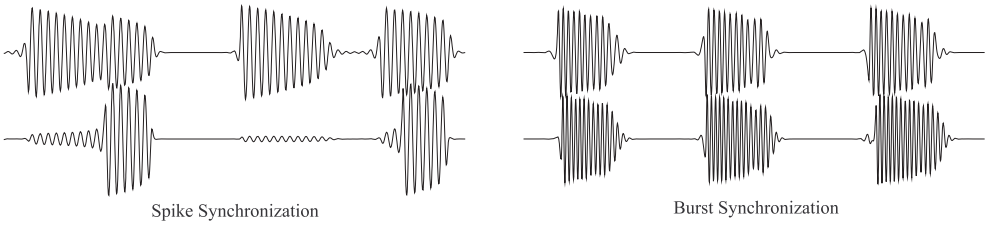

Fig. 4.1 *Various regimes of synchronization of bursters.*

parameters b_i, c_i, d_i, and u_i, which could be chosen so that burst synchronization is not achieved.

4.2. Burst Synchronization. Studying burst synchronization in a network of $n > 2$ Bautin bursters is an important but difficult problem that has not been tackled yet. Even the case of two identical bursters poses many problems, which we do not address in this paper. Instead, we discuss a few obvious facts and leave detailed analysis to the reader.

We distinguish two cases:

- instantaneous burst synchronization via destruction of the slow passage effect,
- burst synchronization via fast threshold modulation.

The first case occurs when each individual burster exhibits the slow passage effect (Nejshtadt (1985); Baer, Erneux, and Rinzel (1989)). The second case covers the remaining possibilities.

Consider a network of two identical bursters having the term $-|z_i|^2$ in the slow subsystem. Using suitable rescaling of parameters, variables, and time τ, we transform the canonical model (3.2) into the form

$$\begin{aligned} z_i' &= (1+\mathrm{i}\beta)u_i z_i + (2+\mathrm{i}\gamma)z_i|z_i|^2 - (1+\mathrm{i}\sigma)z_i|z_i|^4 + \sum_{j=1}^{n} c_{ij} z_j, \\ u_i' &= \eta(a - |z_i|^2). \end{aligned}$$

We use polar coordinates $z_i = r_i e^{\mathrm{i}\varphi_i}$ to rewrite the system above in the form

$$\begin{aligned} r_i' &= u_i r_i + 2r_i^3 - r_i^5 + \sum_{j=1}^{n} s_{ij} r_j \cos(\psi_{ij} + \varphi_j - \varphi_i), \\ \varphi_i' &= \beta u_i + \gamma r_i^2 - \sigma r_i^4 + \frac{1}{r_i}\sum_{j=1}^{n} s_{ij} r_j \sin(\psi_{ij} + \varphi_j - \varphi_i), \\ u_i' &= \eta(a - r_i^2). \end{aligned}$$

Below we assume that $0 < a < 1$ so that the bursters have behavior with alternating active and silent phases, as in the upper part of Figure 2.2.

Instantaneous Synchronization via the Slow Passage Effect. One of the most striking features of weakly connected Bautin bursters is that burst synchronization may be achieved almost instantaneously. Let us elaborate. Suppose that both bursters are quiescent, that is, $r_1 \approx 0$ and $r_2 \approx 0$, but the slow variables u_1 and u_2 have different values so that the bursters would start firing at different times if they were uncoupled. Without loss of generality we may assume that $u_1 < u_2$ at the initial moment $t_0 = 0$;

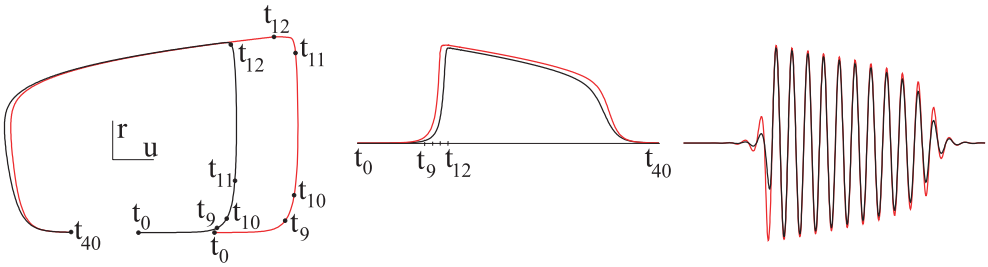

Fig. 4.2 *Two Bautin bursters synchronize almost instantaneously even when they start from essentially different initial conditions. Continuous (dashed) curve is the solution of the first (second) burster. Filled circles denote solutions at the moments $t_k = k$. Parameters:* $a = 0.7,\ \eta = 0.1,\ c_{12} = c_{21} = 1/4,\ u_1(0) = -0.3, u_2(0) = -0.25$.

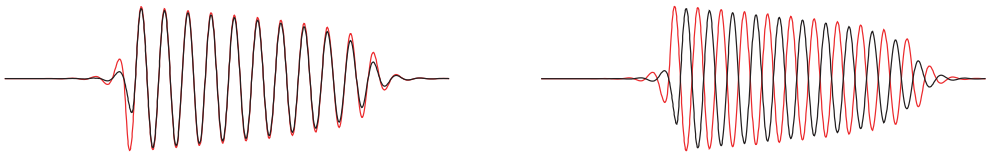

Fig. 4.3 *Illustration to Corollary* 4.3. *Left:* $c_{12} = c_{21} = 1/4$. *Right:* $c_{12} = c_{21} = -1/4$. *Other parameters are as in Figure* 4.2.

see Figure 4.2. Suppose the second burster starts firing, that is, becomes active. After r_2 jumps to the upper branch, activity of the first burster is governed by the system

$$\begin{aligned} r_1' &= u_1 r_1 + 2r_1^3 - r_1^5 + s_{12} r_2 \cos(\psi_{12} + \varphi_2 - \varphi_1), \\ \varphi_1' &= \beta u_1 + \gamma r_1^2 - \sigma r_1^4 + s_{12} \tfrac{r_2}{r_1} \sin(\psi_{12} + \varphi_2 - \varphi_1), \\ u_1' &= \eta(a - r_1^2). \end{aligned}$$

Suppose the first burster continues to be quiescent. Since $r_1 \ll r_2$ in this case, we conclude that

$$\varphi_1(\tau) \to \varphi_2(\tau) + \psi_{12} \tag{4.1}$$

very quickly (hence the term "natural phase difference" for ψ_{12}). Since $\cos(\psi_{12} + \varphi_2(\tau) - \varphi_1(\tau)) \to 1$ with the same rate, the system above reduces to

$$\begin{aligned} r_1' &= u_1 r_1 + 2r_1^3 - r_1^5 + s_{12} r_2, \\ u_1' &= \eta(a - r_1^2). \end{aligned} \tag{4.2}$$

Notice that this system depends only on the synaptic amplitude $s_{12} = |c_{12}| \geq 0$ and does not depend on the natural phase difference $\psi_{12} = \operatorname{Arg} c_{12}$. We combine (4.1) and (4.2) to reach the following conclusion.

COROLLARY 4.3. *Whether connections between local Bautin bursters are excitatory or inhibitory may not affect burst synchronization but does affect spike synchronization; see Figure* 4.3.

Let us contrast the nullclines of the system (4.2) above for $r_2 = 0$ and $r_2 \neq 0$; see Figure 4.4. If the second burster were silent, the nullcline would be N_0 and the first burster would continue to be quiescent due to the slow passage effect (Nejshtadt

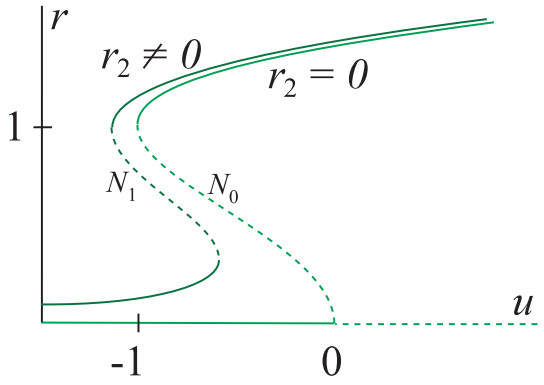

Fig. 4.4 *Nullclines N_0 and N_1 of the system (4.2) for $r_2 = 0$ and $r_2 = 1$, respectively (value $s_{12} = 1/8$ was used).*

(1985)) depicted in the upper part of Figure 2.2. Since $r_2 \neq 0$, the system above has nullcline of the form N_1. Obviously, r_1 cannot remain near the origin and jumps to the upper branch of N_1 for all values of u_1 greater than a certain (negative) value that depends on s_{12}. This process takes $\mathcal{O}(1)$ units of time and looks instantaneous on the larger time scale of order $\mathcal{O}(1/\eta)$ corresponding to the period of each burst. This explains the nearly instantaneous onset of firing by both bursters that we see in Figure 4.2.

In-Phase versus Out-of-Phase Synchronization. Unlike coupled phase oscillators, relaxation oscillators synchronize in-phase even when they have essentially different frequencies. A network of Bautin bursters is not an exception.

Remark 4.4. In-phase synchronization is usually encountered in a network of quantitatively different bursters, whereas out-of-phase synchronization is difficult to achieve.

Indeed, from Figure 4.2 it follows that two bursters synchronize almost instantaneously even when they have essentially different values of slow variables u_1 and u_2. The difference may be due to distinct initial conditions as well as distinct quantitative features. For example, if one of the bursters, say the first one, has a longer interburst period, it tends to fall behind the second burster during the quiescent state even when they start from identical initial conditions. If the quantitative distinction is not too sharp, the first burster would be in the zone of the slow passage effect ($u_1 > 0$) by the time the second burster starts to fire. Since the slow passage effect is sensitive to perturbations, firing of the second burster destroys the effect and elicits an almost instantaneous response from the first burster. Even though there is an $\mathcal{O}(1)$ delay in the response, which may be considered as a phase shift, it is negligible on the large time scale $\mathcal{O}(1/\eta)$, since it constitutes only a small ($\eta \ll 1$) fraction of the period of a burst; see the right-hand side of Figure 4.2.

A word of caution is in order: The slow passage effect is sensitive to noise and nonsmoothness of dynamics (Nejshtadt (1985)). Therefore, however ubiquitous it might seem in computer simulations, it has never been seen in real neurons.

Fast Threshold Modulation. If there are many simultaneously active bursters in a network, if the small-order term $\mathcal{O}(\sqrt[4]{\varepsilon})$ in the canonical model (3.2) is not negligible, or if there is noise in the system, then each nullcline looks qualitatively like N_1 depicted in Figure 4.4, not like N_0. In this case we may treat the bursters as being strongly

connected Bonhoeffer–Van der Pol-type relaxation oscillators, which are studied, e.g., by Belair and Holmes (1984), Grasman (1987), Kopell and Somers (1995), Skinner, Kopell, and Marder (1994), Somers and Kopell (1993), (1995), Storti and Rand (1986), and others. In particular, we may use the *fast threshold modulation* theory (Somers and Kopell (1993)) to study the canonical model (3.2).

Whether or not the bursters synchronize in-phase depends on the relative rates of the slow variable on the lower and upper branches of the nullcline N_1. For example, when a is near 0, variable u increases slowly during the silent phase and decreases quickly during the active phase, which leads to the in-phase synchronization via fast threshold modulation. An out-of-phase synchronization is difficult to achieve in this case even when the bursters are quantitatively different. In contrast, when a is near 1, the rate during the active phase may be slower than that during the silent phase, which may lead to desynchronization even when the bursters are identical. These informal considerations can be made precise when $|c_{ij}|$ are not very large (Izhikevich (2000c)).

5. FitzHugh–Rinzel Model. It should be noted that our analysis above was local; that is, the reduction of an arbitrary Bautin burster to the canonical model was proved only in a small neighborhood of the Bautin point. Thus, we may not make any global conclusions without further analysis. In this section we use the FitzHugh–Rinzel model of elliptic bursters (Rinzel (1987)) to evaluate how studying local Bautin bursters contributes to our understanding of global elliptic bursting.

The FitzHugh–Rinzel model takes the form

$$\begin{aligned} \dot{v} &= v - v^3/3 - w + y + I, \\ \dot{w} &= \delta(a + v - bw), \\ \dot{y} &= \mu(c - v - dy), \end{aligned}$$

where $I = 0.3125$, $a = 0.7$, $b = 0.8$, $c = -0.775$, $d = 1$, $\delta = 0.08$, and $\mu = 0.0001$ are the values used by Rinzel (1987). This system can be written in the form (1.1) if we denote $x = (v, w) \in \mathbb{R}^2$. Note that the fast subsystem is the classical FitzHugh–Nagumo equation (FitzHugh (1961)), which we discussed in section 1.4 (see also Figure 5.1), and the slow subsystem is one-dimensional. The FitzHugh–Rinzel model with the parameters defined above produces singular elliptic bursting with large amplitude spikes; see Figure 5.2. Therefore, one would expect the behavior of the FitzHugh–Rinzel model to be quite different from that of the canonical model (2.1).

Another feature of the FitzHugh–Rinzel model is that the attraction to the unique equilibrium is relatively weak. As was pointed out by Rinzel (1987), this may decrease the slow passage effect or even lead to premature reentry into the active phase; see Figure 5.3. The latter likely contributes to the apparent irregularity of bursting.

We conclude by noting that the FitzHugh–Rinzel model with the choice of the parameters above could by no means be classified as a local Bautin burster. This sets fair grounds for our comparisons below. In addition, we use Morris–Lecar and Hodgkin–Huxley models to illustrate some results.

5.1. Onset and Termination of Bursting. Let us test how studying the canonical model (2.1) contributes to our understanding of elliptic bursting. In particular, let us compare how periodic bursting appears and disappears when we change parameters of the slow subsystem. Parameter a in the canonical model corresponds (up to a rescaling) to the parameter c in the FitzHugh–Rinzel model. Decreasing a leads to longer interburst intervals but relatively constant burst duration. Increasing a leads to shorter interburst intervals until the periodic bursting becomes tonic spiking; see

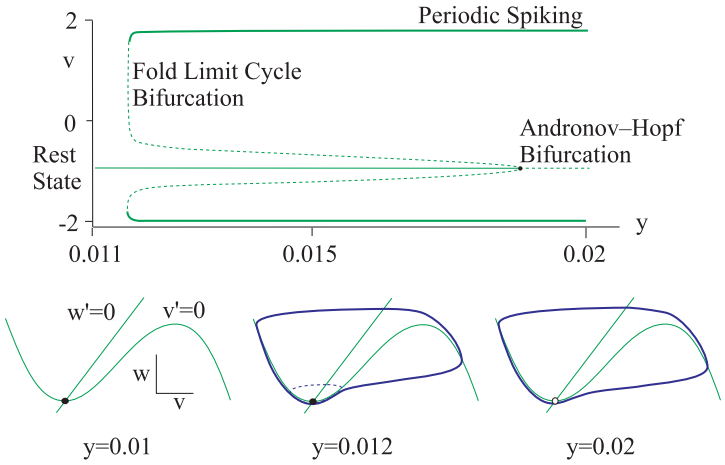

Fig. 5.1 *Bifurcations in the FitzHugh–Rinzel elliptic burster.*

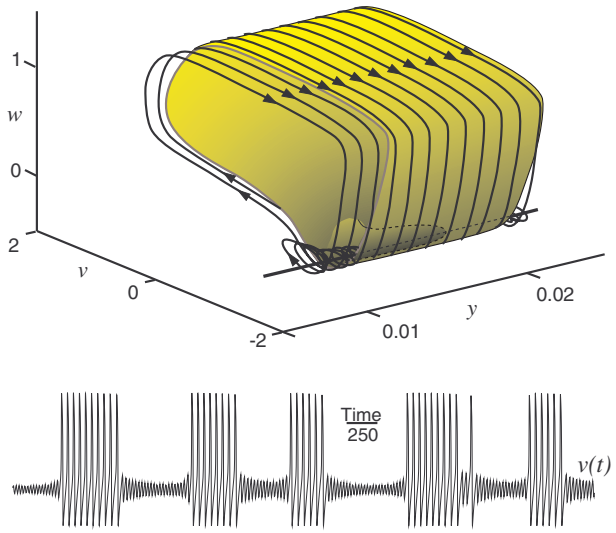

Fig. 5.2 *FitzHugh–Rinzel elliptic ("subHopf/fold cycle") burster.*

Figure 2.2. Similar behavior is observed in the FitzHugh–Rinzel model and in the Wu–Baer model (1997) with the exception that the transition from periodic bursting to tonic spiking is erratic; see Figure 5.4.

5.2. Spike Synchronization. Let us consider a network of FitzHugh–Rinzel elliptic bursters, which we take in the form

$$\begin{aligned}
\dot{v}_i &= v_i - v_i^3/3 - w_i + y_i + I + \sum_{j=1}^{n} s_{ij} v_j, \\
\dot{w}_i &= \delta_i(a + v_i - b w_i), \\
\dot{y}_i &= \mu(c - v_i - d y_i).
\end{aligned}$$

Parameters s_{ij} determine the strength and sign of connections between the bursters.

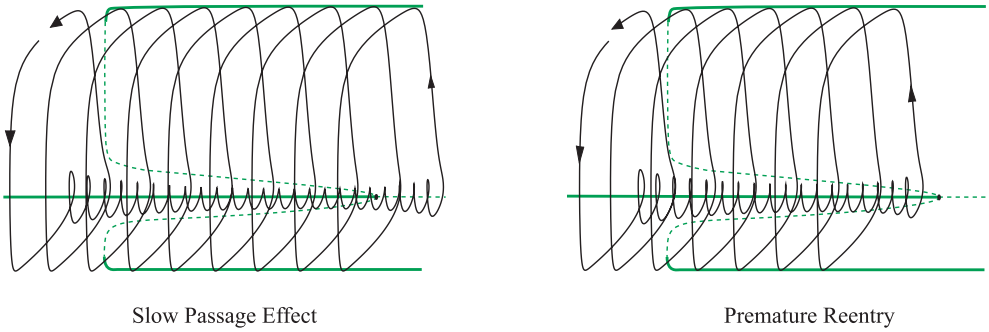

Fig. 5.3 *Slow passage effect and premature reentry into the active phase in the FitzHugh–Rinzel model.*

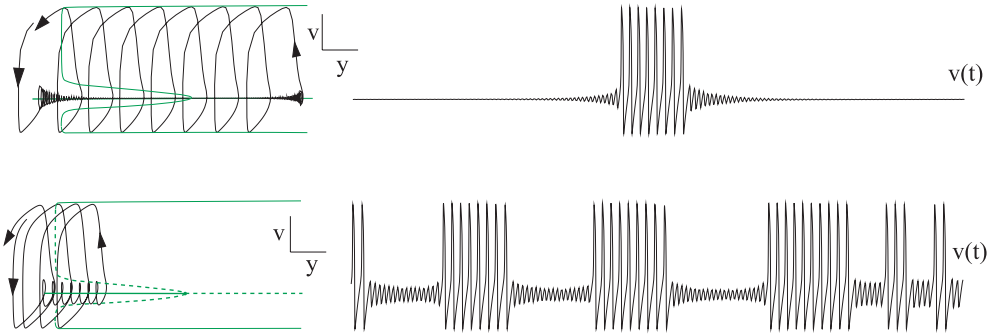

Fig. 5.4 *Solutions of the FitzHugh–Rinzel model for* $c = -0.9$ *(upper part) and* $c = -0.75$ *(lower part).*

We select $c = -0.9$ so that each burster behaves as depicted in the upper part of Figure 5.4. We use $n = 2$ and such initial conditions that the second burster, if uncoupled from the first one ($s_{21} = 0$), starts to fire with a considerable delay; see the upper part of Figure 5.5. When weakly coupled ($|s_{ij}| = 0.002$), the bursters tend to synchronize regardless of the sign of the connection; see the rest of Figure 5.5. The type of spike synchronization (in-phase, anti-phase, etc.) depends on whether connections are excitatory or inhibitory, which is in total agreement with Corollary 4.3 and Figure 4.3. In Figure 5.6 we illustrate this result using Hodgkin–Huxley and Morris–Lecar bursters. A new feature of the FitzHugh–Rinzel and Hodgkin–Huxley models is a considerable prolongation of the active phase when the connections are inhibitory. We do not see this in the canonical model.

5.3. FM Interactions. To check how interactions between the FitzHugh–Rinzel bursters depend on the relation between their frequencies, we consider a pair of such bursters with $s_{12} = 0$ and $s_{21} = 0.002$. Thus, the first burster is presynaptic and the second one is postsynaptic. We vary parameter δ_1 to control the spiking frequency of the presynaptic burster. The other parameters are unchanged. We choose initial conditions so that the presynaptic burster begins its active phase at time $t = 0$, whereas the postsynaptic one, if uncoupled, becomes active with a substantial delay (more than 1000 units of time).

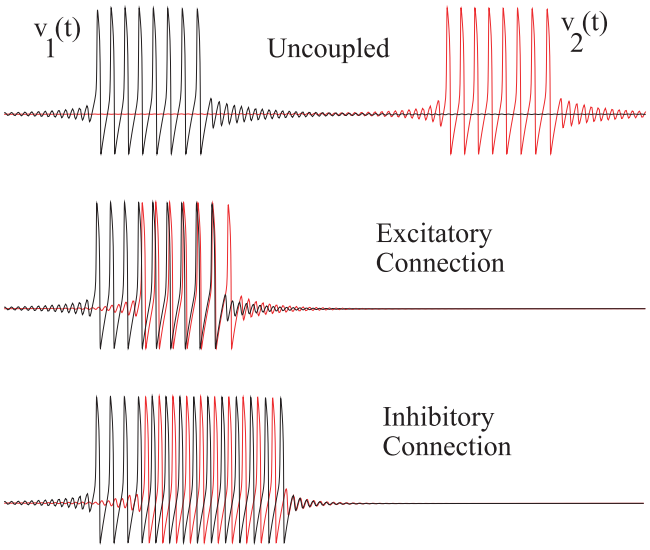

Fig. 5.5 *Solutions of two weakly coupled FitzHugh–Rinzel bursters. Upper part:* $s_{12} = s_{21} = 0$. *Middle part:* $s_{12} = s_{21} = 0.002$. *Lower part:* $s_{12} = s_{21} = -0.002$.

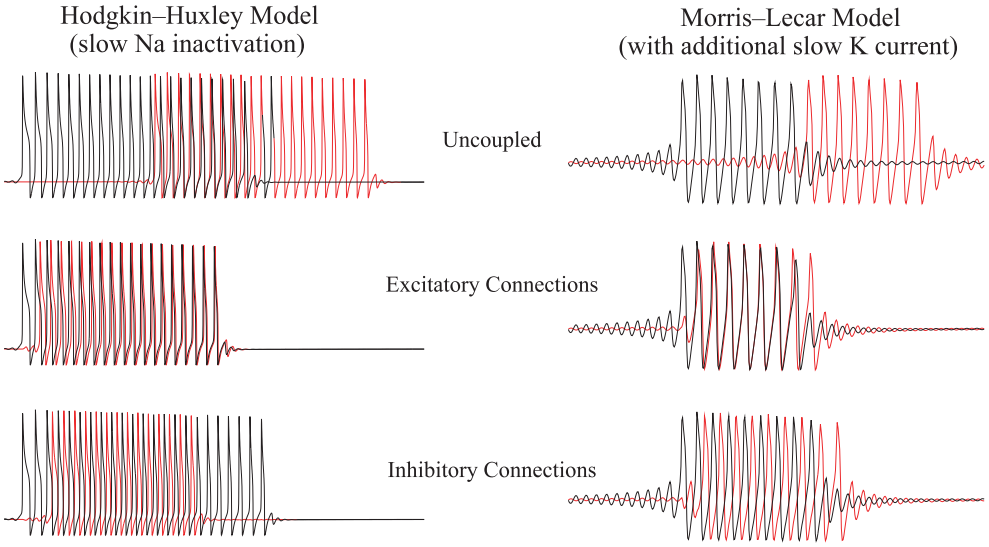

Fig. 5.6 *Spike synchronization between two coupled Hodgkin–Huxley bursters (both from Figure* 1.10a*) and Morris–Lecar bursters (both from Figure* 1.11*).*

Since the frequency of large amplitude spiking in a relaxation oscillator differs substantially from the frequency of small-amplitude oscillation near the equilibrium, none of the cases depicted in Figure 5.7 corresponds to 1:1 locking. The upper part of the figure corresponds to 1:2 locking; that is, the membrane potential of the postsynaptic burster produces two small-amplitude oscillations during each spike of the presynaptic one. Apparently, a few spikes are enough to destabilize the postsynaptic

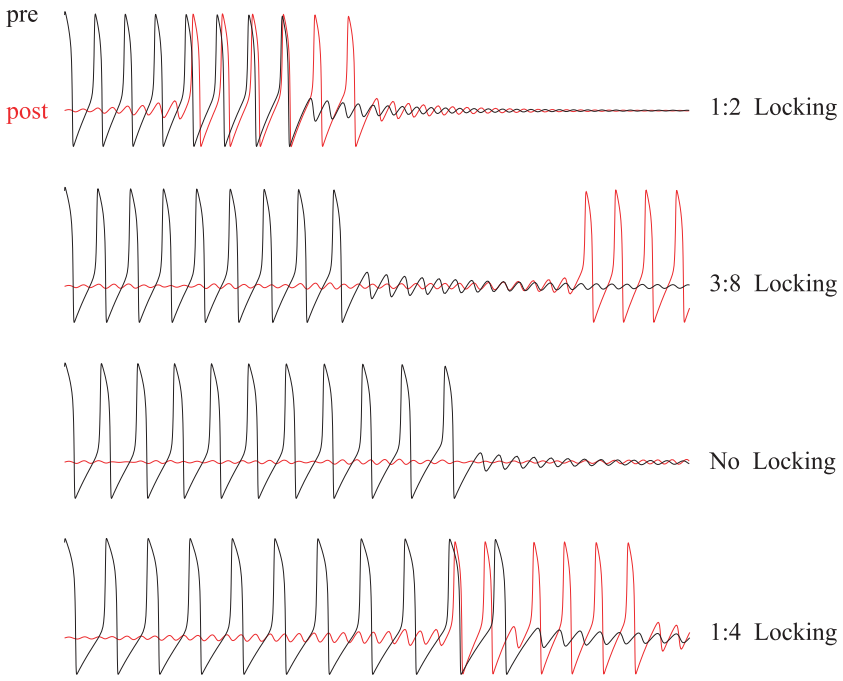

Fig. 5.7 *Frequency modulated (FM) interactions between weakly connected FitzHugh–Rinzel bursters. Parameters:* $I = 0.3125$, $a = 0.7$, $b = 0.8$, $c = -0.9$, $d = 1$, $\mu = 0.0001$, *and* $s_{12} = 0$ *and* $s_{21} = 0.002$. *Simulation time* $t \in [0, 1000]$. *The parameter* δ_1 *was used to control the spiking frequency of the presynaptic burster. From top to the bottom:* $\delta_1 = 0.08,\ 0.07,\ 0.06,\ 0.05$.

burster and make it active. This is not the case in the two middle parts of the figure, even though the presynaptic neuron generates more spikes. At the bottom we depict the case of 1:4 locking, which leads to relatively rapid postsynaptic response.

We see that the Corollary 3.2 is not applicable to elliptic bursters of singular type. A possible explanation would be that local Bautin bursters produce small-amplitude spiking, whereas the FitzHugh–Rinzel bursters produce large amplitude spiking. The actual reason is slightly deeper: the limit cycle corresponding to repetitive spiking has a circle shape in the former case, but it is distorted in the latter case. Such a distortion generates harmonics and subharmonics, which start to play a role in locking behavior. Similar discrepancies can be observed between weakly connected networks near a multiple Andronov–Hopf bifurcation and weakly connected limit cycle (phase) oscillators (Hoppensteadt and Izhikevich (1997)). In order to establish communication, one requires equality of frequencies in the former case, whereas only their resonance is sufficient in the latter.

In Figure 5.8 we repeat a similar experiment using the Morris–Lecar system from Figure 1.11. We can change the frequency of firing of the presynaptic burster (black) by multiplying the right-hand side of the Morris–Lecar system by a constant. We choose the constant so that its frequency of firing is close to the frequency of subthreshold oscillations of the postsynaptic burster (red). We choose the initial conditions so that the postsynaptic burster fires with a significant delay when there are no connections (top voltage trace in Figure 5.8). When the bursters are connected, just a

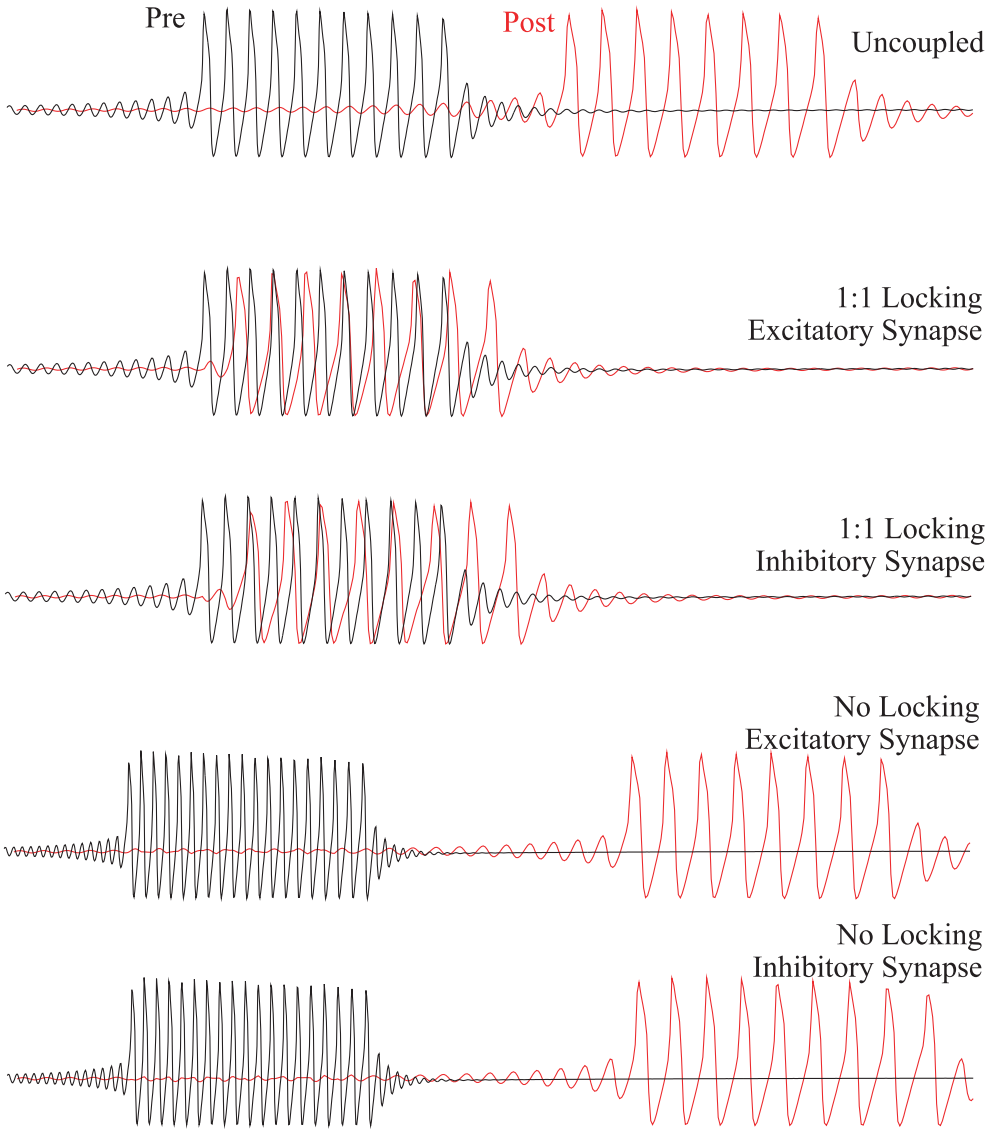

Fig. 5.8 *FM interactions and burst synchronization between two Morris–Lecar neurons from Figure* 1.11. *The presynaptic burster (black) can evoke immediate response in the postsynaptic burster (red) when its frequency of firing equals the frequency of subthreshold oscillation of the postsynaptic burster (*1:1 *locking in the second and third voltage traces). If the frequencies are different, the input from the presynaptic burster is not effective (bottom two voltage traces).*

few excitatory or inhibitory spikes are enough to destabilize the postsynaptic burster. A seemingly counterintuitive phenomenon occurs when we increase the frequency of the presynaptic burster without changing the strength of the synaptic connection: The presynaptic input becomes less effective (bottom two voltage traces in Figure 5.8), despite the fact that the burster produces more spikes. This occurs because the frequency ratio is no longer 1:1. Thus, the ratio of frequencies plays a crucial role in the synchronization of elliptic bursters.

Finally, notice an important difference between local Bautin bursters and global elliptic bursters: the large-amplitude spiking and the small-amplitude oscillations near the equilibrium have nearly identical frequencies in the former, but may have drastically different frequencies in the latter. Therefore, we must distinguish the interspike frequency and the frequency of small-amplitude membrane oscillations and state an analogue of Corollary 3.2 in the following form.

Remark 5.1. The rate of burst synchronization of weakly connected global elliptic bursters depends on the ratio of the interspike frequency of the presynaptic burster and the frequency of small-amplitude oscillations of the postsynaptic burster. It is fastest when the frequencies are nearly identical, slower when the ratio is near 1:2, even slower for the ratio near 1:3, etc. In contrast, spike synchronization depends on the ratio of interspike frequencies and does not depend on the frequencies of small-amplitude oscillations.

6. Discussion. The main purpose of this paper is to derive a canonical model (2.1) for elliptic bursters of Bautin type and to use it to study nonlinear dynamics and synchronization properties of coupled elliptic bursters.

6.1. Bursters Are Local. A major requirement for such a derivation is that the bursters are local; that is, the transition to periodic spiking (via Andronov–Hopf bifurcation) and back to quiescent state (via fold limit cycle bifurcation) occurs for nearby values of a slow variable. Incidentally, this does not imply that there are only a few spikes during each burst; the slow variable changes so slowly that the fast subsystem has enough time to generate many spikes.

We study the case when the fast subsystem is in a small neighborhood of the Bautin bifurcation point where the Andronov–Hopf and fold limit cycle bifurcation curves meet. This imposes additional restrictions on the elliptic bursters that can be transformed into the canonical form (2.1).

A consequence of being near the Bautin bifurcation point is that the periodic spiking may have small amplitude. In this case the canonical model captures elliptic bursting "in embryo." Nevertheless, it does reflect some qualitative features of global elliptic bursters (see Figure 1.13) provided that no bifurcation occurs while the fast subsystem is pulled out from a small neighborhood of the Bautin point.

6.2. Singular versus Nonsingular Bursters. An important case that is not covered by our analysis is when the fast subsystem has many time scales and generates spikes via relaxation oscillations. In this case an elliptic burster may be singular. A typical example of such a burster is the FitzHugh–Rinzel model that we consider in section 5. Computer simulations of the FitzHugh–Rinzel, Morris–Lecar, and Hodgkin–Huxley models show that local analysis of Bautin bursters provides accurate insight into global behavior of singular elliptic bursters.

6.3. Hysteresis. It is remarkable that the slow variable in the canonical model (2.1) is one-dimensional and that it oscillates via a hysteresis. Indeed, the slow variable in the original burster (1.1) is multidimensional and our only assumption about the slow dynamics is that it has a stable equilibrium. We do not assume anything about hysteresis, but it seems to emerge naturally during the canonical model derivation. Thus, we come to the conclusion that hysteresis behavior of a slow subsystem in elliptic bursters is a natural property, not an artifact of "minimal" models.

6.4. Biological Plausibility. An advantage of studying the canonical model (2.1) is that it is simpler than most systems of the form (1.1). One may argue that this is not an advantage at all, because

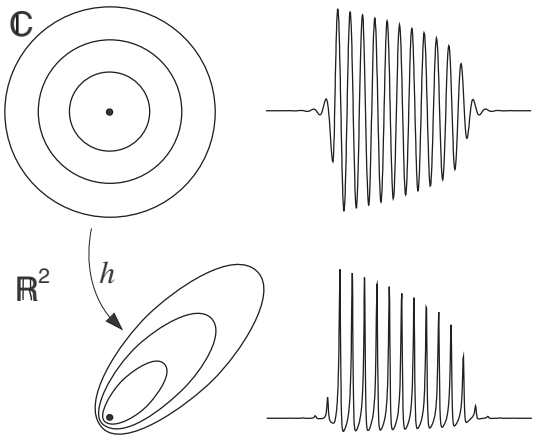

Fig. 6.1 *A homeomorphism $h : C \to \mathbb{R}^2$ may transform solutions of the canonical model to a more "biologically plausible" form. See text for details. (Simulations are performed for $h(z) = z|z|/(1.1|z| - \mathrm{Re}\,(ze^{-\mathrm{i}\pi/4}))$, $a = 0.7$, and $\eta = 0.1$.)*

- multidimensional systems of the form (1.1) describing elliptic bursters are more biologically plausible than the canonical model because they may take into account many physiological facts that are hard to identify in (2.1); and
- solutions of the canonical model have a simple shape that is different from the familiar "Hodgkin–Huxley-type" shape that we see in electrophysiological experiments (contrast the upper and lower parts of Figure 6.1).

First, each local Bautin burster of the form (1.1) can be transformed into the canonical model by an appropriate *continuous* change of variables (this is the definition of a canonical model). The form of the canonical model captures the essence of Bautin bursting that is present in all (1.1), while the parameters of the canonical model capture the particulars of each individual burster. The fact that we do not have complete and precise information about all neurophysiological processes taking place during bursting means that we do not know and probably will never know the exact form of the functions f and g in (1.1) (we do not even know the dimension of the vectors x and y), which is frustrating. The same fact in terms of the canonical model means that we do not know the exact values of the parameters a and η, which is much less frustrating since we can study it for all a and η. This is the reason we are interested in canonical models (see the book by Hoppensteadt and Izhikevich (1997) for more examples of canonical models).

Next, note that any system that is topologically equivalent to the canonical model (2.1) is a canonical model too. Therefore, if one does not like the shape of the spiking in (2.1), one could take a homeomorphism $h : \mathbb{C} \to \mathbb{R}^2$ that distorts nice periodic orbits corresponding to repetitive spiking into something less nice but more "biologically plausible." Let $w = h(z)$; then the canonical model is transformed into a system of the form

$$w' = Dh(h^{-1}(w))[(u + \mathrm{i}\omega)h^{-1}(w) + 2h^{-1}(w)|h^{-1}(w)|^2 - h^{-1}(w)|h^{-1}(w)|^4],$$
$$u' = \eta(a - |h^{-1}(w)|^2),$$

which produces spikes of the desired shape; see the illustration in Figure 6.1. Its behavior is exactly the same as that of (2.1), since they are topologically equivalent, but the system above is less mathematically tractable.

6.5. Weakly Connected Networks. When we derive the canonical model for weakly connected Bautin bursters, we do not assume that they are connected exclusively via fast variables; see (3.1). Nevertheless, the canonical model (3.2) is connected only via fast variables. Therefore, the connections "fast → slow," "slow → slow," and "slow → fast" can be removed by an appropriate continuous change of variables; see Theorem 3.1. Since the connections "fast → fast" correspond to interaction via spikes, we speculate that even if two bursters could interact via a nonspiking mechanism, it would be much less effective than spiking interaction. Similar conclusions arise in studying weakly connected relaxation oscillators (Hoppensteadt and Izhikevich (1997, section 6.9)).

6.6. FM Interactions. A seemingly counterintuitive fact is that weakly connected local Bautin bursters do not interact unless they have matching interspike frequencies (Corollary 3.2). That is, synaptic transmission between a pair of bursting neurons having distinct interspike frequencies averages to zero, and hence it is functionally insignificant. Since the significance of interactions between bursters is determined by the interspike frequency, we refer to such interactions as being frequency modulated (FM).

The requirement that the frequencies must coincide is a consequence of the fact that the spiking of the presynaptic burster and the small-amplitude oscillations near the equilibrium of the postsynaptic burster have circular shape. When the spiking has a distorted shape, as in the FitzHugh–Rinzel or Morris–Lecar model, then the requirement that the frequencies be nearly identical is replaced by the requirement that the frequencies be nicely commensurable (see Hoppensteadt and Izhikevich (1997, Chapter 9)); that is, the interactions are most effective for nearly identical frequencies, less effective when the frequency ratio is near 1:2, even less effective for the ratio 1:3, etc., and negligible when the ratio is near i:j for some large, relatively prime integers i and j. Here "near" means ε-close, where $\varepsilon \ll 1$ is the strength of connections.

This result is no longer counterintuitive if we recall how the slow passage effect can be affected by noise. Baer, Erneux, and Rinzel (1989) showed that the noise reduces the slow passage effect through resonance; that is, the noise should have frequencies in its power spectrum that are integer multiples of the natural frequency Ω at the Andronov–Hopf bifurcation. If we treat a weak input to a burster as a noise, then it is clear that the input is functionally insignificant unless it has resonant frequencies. Llinás (1988) suggested using the term *resonator* for such FM interacting neurons. In the tutorial paper (Izhikevich (2000a)) we review how resonance behavior appears in neural systems near Andronov–Hopf bifurcation. (Such neural systems exhibit damped or sustained oscillations of membrane potential.)

An important difference between local Bautin bursters and global elliptic bursters is that the spiking and the small-amplitude oscillations near the equilibrium have nearly identical frequencies in the former but may have drastically different frequencies in the latter. As a result, we have to be more specific when we compare frequencies of oscillations of (global) elliptic bursters. For example, burst synchronization depends on the ratio of the interspike frequency of the presynaptic burster and the frequency of small-amplitude (subthreshold) oscillations of the postsynaptic one. In contrast, spike synchronization depends exclusively on the ratio of interspike frequencies.

6.7. Rate of Synchronization. The rate of convergence to attractors in weakly connected networks is very slow; namely, it is of order $\varepsilon \ll 1$, where ε is the strength of connections (Hoppensteadt and Izhikevich (1997)). For example, a weakly connected

oscillatory network needs as many as $\mathcal{O}(1/\varepsilon)$ cycles to synchronize[1] regardless of whether each element is a relaxation oscillator (Izhikevich (2000c)) or a smooth limit cycle oscillator. This is the major source of criticism of weakly connected models, since the slow rate of convergence contradicts, e.g., the CPG behavior in the lamprey, which is characterized by a strong rate of convergence to an attractor (see, e.g., Kopell (1995), Somers and Kopell (1995), and Williams and Sigvardt (1995)).

Our analysis of weakly connected bursters suggests that the discrepancy in rates of convergence is not due to the assumption of weakness of connections, but due to the assumption that each segment of lamprey spinal cord can be modeled by an oscillator. If we model it by a burster, which it is, then the rate of convergence to an attractor looks "fast" compared to the interburst period despite the fact that the bursters are weakly connected. Indeed, it takes $\mathcal{O}(1/\varepsilon)$ spikes to produce $\mathcal{O}(1)$ changes in the activity of a postsynaptic segment, but there are as many as $\mathcal{O}(1/(\varepsilon\eta))$ spikes in each burst. Therefore, one burst is usually enough for two segments to lock. Another way to explain this is to note that locking of two segments requires $\mathcal{O}(1/\varepsilon)$ units of time, but each burst lasts $\mathcal{O}(1/(\varepsilon\eta))$ units. Therefore, locking of segments looks instantaneous on the time scale of interburst intervals, even though it takes the same $\mathcal{O}(1/\varepsilon)$ time to achieve.

We see that the apparent difference in convergence rates of weakly connected limit-cycle oscillators and bursters is a matter of semantics, since the former is compared with the inter*spike* intervals whereas the latter is compared with the inter*burst* intervals.

6.8. Spike versus Burst Synchronization. We see that it is important to distinguish two rhythmic processes: periodic spiking and periodic bursting. Therefore, there are at least two regimes of synchronization; see Figure 4.1. Spike synchronization is difficult to achieve unless some additional conditions are imposed, e.g., those in Theorem 4.1. In contrast, burst synchronization is difficult to avoid. Moreover, substantial changes in the parameters of the system, which would lead to the disappearance of synchronization or at least to a considerable phase shift if we modeled weakly connected smooth limit cycle (phase) oscillators, do not produce any significant lag between bursts. That is, burst synchronization tends to be in-phase despite any quantitative differences between the bursters. In this sense, behavior of weakly connected local Bautin bursters resembles that of *strongly connected* relaxation oscillators, as described by Somers and Kopell (1993), (1995).

An odd feature of weakly connected elliptic bursters is that both excitatory and inhibitory synaptic connections may lead to in-phase burst synchronization. Even though the sign of the synapse affects spike synchronization, i.e., whether it is in-phase, anti-phase, or just out-of-phase (see Corollary 4.3), it seems to be irrelevant to burst synchronization in many instances.

Acknowledgments. The author acknowledges Frank Hoppensteadt, whose collaboration and constant support have been invaluable. This paper was conceived during a meeting with Thomas Erneux in Snowbird, Utah, in 1997. Bard Ermentrout pointed out the importance of distinguishing spike and burst synchronization. Many discussions with Steve Baer helped to improve the quality of the manuscript.

[1] By synchronization we mean here convergence to a small but finite neighborhood of an appropriate attractor, which takes $\mathcal{O}(1)$ units of slow time τ and/or $\mathcal{O}(1/\varepsilon)$ units of normal time t. Complete convergence to the attractor is an asymptotic process that requires an infinite amount of time unless the system is non-Lipchitz or the initial state is on the attractor.

In particular, he suggested using the FitzHugh–Rinzel model. Special thanks also go to Arthur Sherman, who made an excellent choice of peer reviewers whose criticism and suggestions helped to improve the quality of the manuscript. The original paper was written while the author was with the Center for Systems Science at Arizona State University. The research was supported in part by the NSF grant "Canonical Models for Mathematical Neuroscience," DMS-9805544. Revisions and simulations included in the present paper were carried out as part of the theoretical neurobiology program at The Neurosciences Institute, which is supported by the Neurosciences Research Foundation.

REFERENCES

V. I. Arnold, V. S. Afrajmovich, Yu. S. Il'yashenko, and L. P. Shil'nikov (1994), *Bifurcation theory*, in Dynamical Systems V. Bifurcation Theory and Catastrophe Theory, V. I. Arnold, ed., Springer-Verlag, New York.

S. M. Baer and T. Erneux (1986), *Singular Hopf bifurcation to relaxation oscillations*, SIAM J. Appl. Math., 46, pp. 721–739.

S. M. Baer and T. Erneux (1992), *Singular Hopf bifurcation to relaxation oscillations* II, SIAM J. Appl. Math., 52, pp. 1651–1664.

S. M. Baer, T. Erneux, and J. Rinzel (1989), *The slow passage through a Hopf bifurcation: Delay, memory effects, and resonance*, SIAM J. Appl. Math., 49, pp. 55–71.

J. Belair and P. Holmes (1984), *On linearly coupled relaxation oscillations*, Quart. Appl. Math., 42, pp. 193–219.

R. Bertram, M. J. Butte, T. Kiemel, and A. Sherman (1995), *Topological and phenomenological classification of bursting oscillations*, Bull. Math. Biol., 57, pp. 413–439.

R. M. Borisyuk and A. B. Kirillov (1992), *Bifurcation analysis of a neural network model*, Biological Cybernetics, 66, pp. 319–325.

W. Eckhaus (1983), *Relaxation oscillations including a standard chase of French ducks*, in Asymptotic Analysis II, Lecture Notes in Math. 985, Springer-Verlag, New York, pp. 432–449.

G. B. Ermentrout and N. Kopell (1986a), *Parabolic bursting in an excitable system coupled with a slow oscillation*, SIAM J. Appl. Math., 46, pp. 233–253.

G. B. Ermentrout and N. Kopell (1986b), *Subcellular oscillations and bursting*, Math. Biosci., 78, pp. 265–291.

R. FitzHugh (1961), *Impulses and physiological states in models of nerve membrane*, Biophysical Journal, 1, pp. 445–466.

J. Grasman (1987), *Asymptotic Methods for Relaxation Oscillations and Applications*, Springer-Verlag, New York.

A. L. Hodgkin and A. F. Huxley (1954), *A quantitative description of membrane current and application to conduction and excitation in nerve*, Journal Physiol., 117, pp. 500–544.

F. C. Hoppensteadt and E. M. Izhikevich (1996a), *Synaptic organizations and dynamical properties of weakly connected neural oscillators:* I. *Analysis of canonical model*, Biological Cybernetics, 75, pp. 117–127.

F. C. Hoppensteadt and E. M. Izhikevich (1996b), *Synaptic organizations and dynamical properties of weakly connected neural oscillators.* II. *Learning of phase information*, Biological Cybernetics, 75, pp. 129–135.

F. C. Hoppensteadt and E. M. Izhikevich (1997), *Weakly Connected Neural Networks*, Springer-Verlag, New York.

F. C. Hoppensteadt and E. M. Izhikevich (1998), *Thalamo-cortical interactions modeled by weakly connected oscillators: Could the brain use FM radio principles?*, BioSystems, 48, pp. 85–94.

E. M. Izhikevich (1998), *Supercritical Elliptic Bursting and the Slow Passage Effect*, preprint.

E. M. Izhikevich (1999), *Weakly connected quasiperiodic oscillators, FM interactions, and multiplexing in the brain,* SIAM J. Appl. Math., 59, pp. 2193–2223.

E. M. Izhikevich (2000a), *Neural excitability, spiking, and bursting*, Int. J. Bifur. Chaos, 10, pp. 1171–1266.

E. M. Izhikevich (2000b), *Subcritical elliptic bursting of Bautin type*, SIAM J. Appl. Math., 60, pp. 503–535.

E. M. Izhikevich (2000c), *Phase equations for relaxation oscillators*, SIAM J. Appl. Math., 60, pp. 1789–1804.

N. Kopell (1995), *Chains of coupled oscillators*, in Brain Theory and Neural Networks, M.A. Arbib, ed., MIT Press, Cambridge, MA.

N. Kopell and D. Somers (1995), *Anti-phase solutions in relaxation oscillators coupled through excitatory interactions*, J. Math. Biol., 33, pp. 261–280.

Yu. Kuznetsov (1995), *Elements of Applied Bifurcation Theory*, Springer-Verlag, New York.

R. R. Llinás (1988), *The intrinsic electrophysiological properties of mammalian neurons: Insights into central nervous system function*, Science, 242, pp. 1654–1664.

B. L. McNaughton, C. A. Barnes, and P. Andersen (1981), *Synaptic efficacy and EPSP summation in granule cells of rat fascia dentata studied in vitro*, J. Neurophysiology, 46, pp. 952–966.

C. Morris and H. Lecar (1981), *Voltage oscillations in the barnacle giant muscle fiber*, Biophysical Journal, 35, pp. 193–213.

A. Nejshtadt (1985), *Asymptotic investigation of the loss of stability by an equilibrium as a pair of eigenvalues slowly cross the imaginary axis*, Uspekhi. Mat. Nauk, 40, pp. 190–191.

C. M. Pedroarena, I. E. Pose, J. Yamuy, M. H. Chase, and F. R. Morales (1999), *Oscillatory membrane potential activity in the soma of a primary afferent neuron,* J. Neurophysiology, 82, pp. 1465–1476.

J. Rinzel (1987), *A formal classification of bursting mechanisms in excitable systems*, in Mathematical Topics in Population Biology, Morphogenesis, and Neurosciences, Lecture Notes in Biomath. 71, E. Teramoto and M. Yamaguti, eds., Springer-Verlag, Berlin.

J. Rinzel and Y. S. Lee (1987), *Dissection of a model for neuronal parabolic bursting*, J. Math. Biol., 25, pp. 653–675.

F. K. Skinner, N. Kopell, and E. Marder (1994), *Mechanism for oscillations and frequency control in reciprocally inhibitory model neural networks*, J. Comput. Neurosci., 1, pp. 69–87.

D. Somers and N. Kopell (1993), *Rapid synchronization through fast threshold modulation*, Biological Cybernetics, 68, pp. 393–407.

D. Somers and N. Kopell (1995), *Waves and synchrony in networks of oscillators or relaxation and non-relaxation type*, Phys. D, 89, pp. 169–183.

D. W. Storti and R. H. Rand (1986), *Dynamics of two strongly coupled relaxation oscillators*, SIAM J. Appl. Math., 46, pp. 56–67.

X. J. Wang and J. Rinzel (1995), *Oscillatory and bursting properties of neurons*, in Brain Theory and Neural Networks, M. A. Arbib, ed., MIT Press, Cambridge, MA.

T. L. Williams and K. A. Sigvardt (1995), *Spinal cord of lamprey: Generation of locomotor patterns*, in Brain Theory and Neural Networks, M. A. Arbib, ed., MIT Press, Cambridge, MA.

H.-Y. Wu and S. M. Baer (1997), *Analysis of an excitable dendritic spine with an activity-dependent stem conductance*, J. Math. Biol., 36, pp. 569–592.